SAND2019-10293C

Design Considerations for a High-Temperature Particle Storage Bin

Jeremy Sment,[1, a)] Kevin Albrecht,[2, b)] Mario J. Martinez,[3] and Clifford K. Ho[4]

[1] *Jeremy Sment (MME), Senior Member of Technical Staff – Mechanical Engineering. Sandia National Laboratories, 1515 Eubank Blvd. SE, Albuquerque, NM 87123, USA, +1 505 844 9614*
[2] *Kevin Albrecht (PhD), Senior Member of Technical Staff – Mechanical Engineering. Sandia National Laboratories +1 505 844 5869*
[3] *Mario J. Martinez (PhD), PMTS R&D S&E – Mechanical Engineering, Sandia National Laboratories +1 505 844 8729*
[4] *Clifford K Ho (PhD), Senior Scientist, Sandia National Laboratories, +1 505 844 2384*

[a)]Corresponding author: jsment@sandia.gov
[b)]kalbrech@sandia.gov

Abstract. Solid particle receivers provide an opportunity to run concentrating solar tower receivers at higher temperatures (~800° C) resulting in increased CSP system efficiencies overall. CSP plants with thermal storage have an economic advantage. A flat-bottomed particle storage bin with internal refractory insulation was designed for the 1MW$_t$ Generation 3 Particle Pilot Plant (G3P3) at the National Solar Thermal Test Facility at Sandia National Laboratories. Computational simulations using a cyclic steady-state model were performed to evaluate the effect that form factor (height to diameter ratio) has on thermal losses. A second method has been developed to model heat transfer of particles in funnel flow. Small scale testing was performed to validate the approach.

INTRODUCTION

The peak efficiencies of concentrated solar power (CSP) plants are partly limited by the peak pressures and temperatures that can be handled by the either heat transfer medium such as salts which begin to break down over ~600° C and the receiver pipes which may become damaged if temperatures get too hot. Solid particle receivers provide an opportunity to bypass piping and directly irradiate a curtain of falling ceramic particles. This enables plants to run concentrating solar tower receivers at higher temperatures (~800° C) resulting in increased CSP system efficiencies overall. Particle based heat transfer media also have beneficial characteristics related to thermal storage as the high specific heat and low conductivity create self-insulating behavior and reduce insulation costs.

The National Solar Thermal Test Facility (NSTTF) at Sandia National Laboratories in Albuquerque, NM is designing and de-risking a 1MW$_t$ Generation 3 Particle Pilot Plant (G3P3) with 6 hours of thermal storage. The G3P3 system is vertically integrated into a tower structure. Particles move from the receiver at the top of the ~46 m tower to the hot-storage bin, heat exchanger, and cold-storage bin under the force of gravity before returning to a bucket elevator which lifts the particles back to the top of the tower. The system overview is described in more detail by Clifford K. Ho et al [1].

Figure 1 shows a cross sectional view of the current G3P3 storage bin. The tank is insulated internally with layers of refractory insulation on the side walls and ceramic wool insulation on the ceiling. However, the particles themselves have a specific heat ~1.243 $\frac{J}{kg*K}$ and a conductivity of only 0.35 $\frac{W}{m*K}$ and therefore contribute substantially to the overall thermal resistance of the storage bin [2]. By comparison, the thermal properties of other bin materials at operational temperatures ~600-800° C (873-1073 K) are shown in **TABLE 1**.

Sandia National Laboratories is a multimission laboratory managed and operated by National Technology & Engineering Solutions of Sandia, LLC, a wholly owned subsidiary of Honeywell International Inc., for the U.S. Department of Energy's National Nuclear Security Administration under contract DE-NA0003525.

TABLE 1: approximate specific heat (c_p), conductivity (λ), and thermal expansion (α) coefficients of storage hopper materials at operational temperatures

Material	$c_p\left(\frac{J}{kg \cdot K}\right)$	$\lambda\left(\frac{W}{m \cdot K}\right)$	$\alpha\left(\frac{1}{K}\right)$
High-density refractory	1175	1.53	2.25
Low-density refractory	1386	0.15	1.75
Microporous Insulation	1050	0.05	2.25
Carbon Steel ANSI32	440	43	11.7
CARBO HSP 40/70	1243	0.35	*
Air	1099	0.024	0.007
*coefficient unavailable			

The internally insulated bin is sized for ~162,000 kg of hot particles which includes ~120,000 kg of flowing particles required to provide a 1MW$_t$ duty for 6 hours and ~42,000 kg of stagnant particles that will remain at the bottom of the tank due to the flat-bottomed design. This layer of stagnant particles provides four key advantages: 1, the self-insulating properties of the particles eliminate the need for insulation on the bottom. 2, the formation of the stagnant particles along the drawdown angle eliminates the need to construct an angled hopper capable of supporting loads of this size. 3, the residual particles protect the floor from abrasion due to the impact of high-velocity falling particles thus eliminating the need for a liner capable of surviving impact and high temperatures. 4, the flat-bottom tank causes a funnel-flow condition where there is zero particle motion tangent to the walls. Particles flow away from the wall along the drawdown angle and into a central flow channel whose shape is defined by the material properties of the particles at temperature.

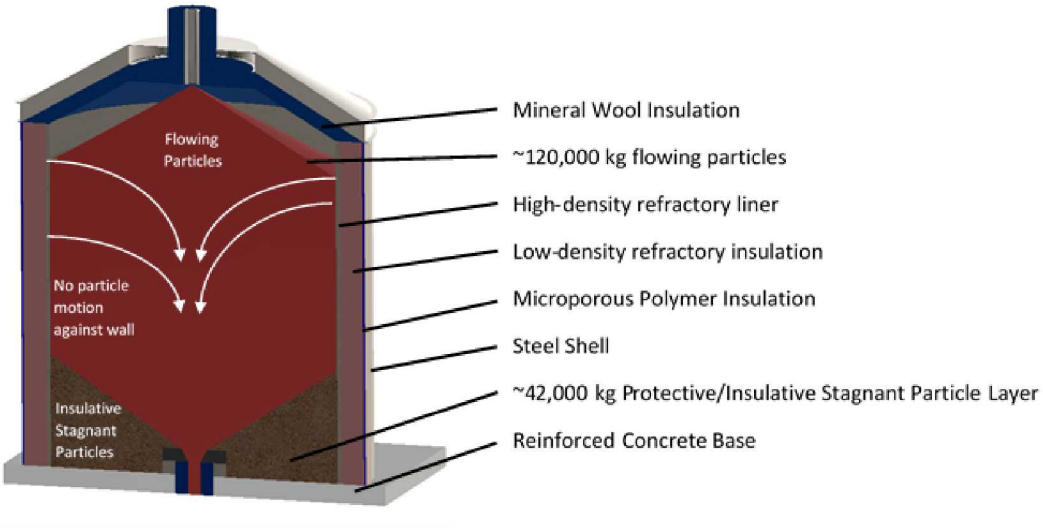

Figure 1. Design of hot particle storage bin for 1 MW$_t$ G3P3 system with 6 MWh$_t$ of storage.

SIMULATIONS OF THERMAL LOSSES

The G3P3 hot storage bin is required to receive particles from the receiver at 800±13° C and must deliver particles to the heat exchanger at 775±10° C. Material selection, additional mass, and thickness of the refractory insulation layers must therefore be chosen to allow particle temperatures at the outlet to drop no more than 22° C during the 8-hour charging, 10- hour required storage period, and the 6-hour discharging phases combined.

Static Quasi-Steady-State Thermal Modeling

Thermal analysis was performed to predict the behavior of temperature and heat loss over time in nominal use conditions where the hopper is filled and discharged daily and the refractory insulation layers of the bin have come to a cyclic steady-state equilibrium. A simulation was conducted where a cold hopper, initially at 25°C, is filled with 800°C particles (instantly) and held for 10 hours. During the storage period, the particles transfer heat to the refractory layers. The particles are then discharged instantly, and the refractory layers lose heat to the environment for the remaining 14 hours. The cycle is repeated until the cyclic differences between temperature and heat loss deltas between charging and discharging phases are negligible (Cyclic Steady-State).

Figure 2 shows the results of a 2D axisymmetric simulation of transient storage bin operation during periodic charging/discharging cycles with height to diameter ratios of the cylindrical portion of 1, 2, and 4. The left axis is temperature with the following: *T_s* being the integrated average temperature of the bulk particles. The daily cycles are identifiable as periodic spikes as particles enter at 1073 K and level off. *T_s_out* is the temperature of the particles where they contact the inner layer of refractory. *T_shell* is the average temperature over the surface of the steel shell. On the right axis is heat flux with *FluxOuter* in W/m^2 indicating the flux out of the system at each time increment the *HeatOuter* in Watts indicating the flux out of the system times the surface area. The bin geometry is selected to minimize surface area of the flowing particle formation. Refractory insulation layers are modeled along the walls, but the floor is comprised only of stagnant particles directly on a concrete slab.

Thermal models illustrate the self-insulating properties of the particles and predict a temperature gradient across the tank with a hot core in the center that remains nearly constant with a relatively steep drop (~300K) near the walls as shown by the lighter red contour in Figure 2a and quantified as in Figure 2b as the difference between *T_s* and *T_s_out*. The results shown in Figure 2b predict a significant amount of heat will be lost to the refractory walls until enough daily charge-discharge cycles have occurred to reach a cyclic steady-state condition. The analysis also illustrates the effectiveness of the stagnant particles as an insulative layer with significantly less heat escapes through the floor (*HeatOuter_conrete*) than through the walls and roof (*HeatOuter_Vertical* and *HeatOuter_roof*).

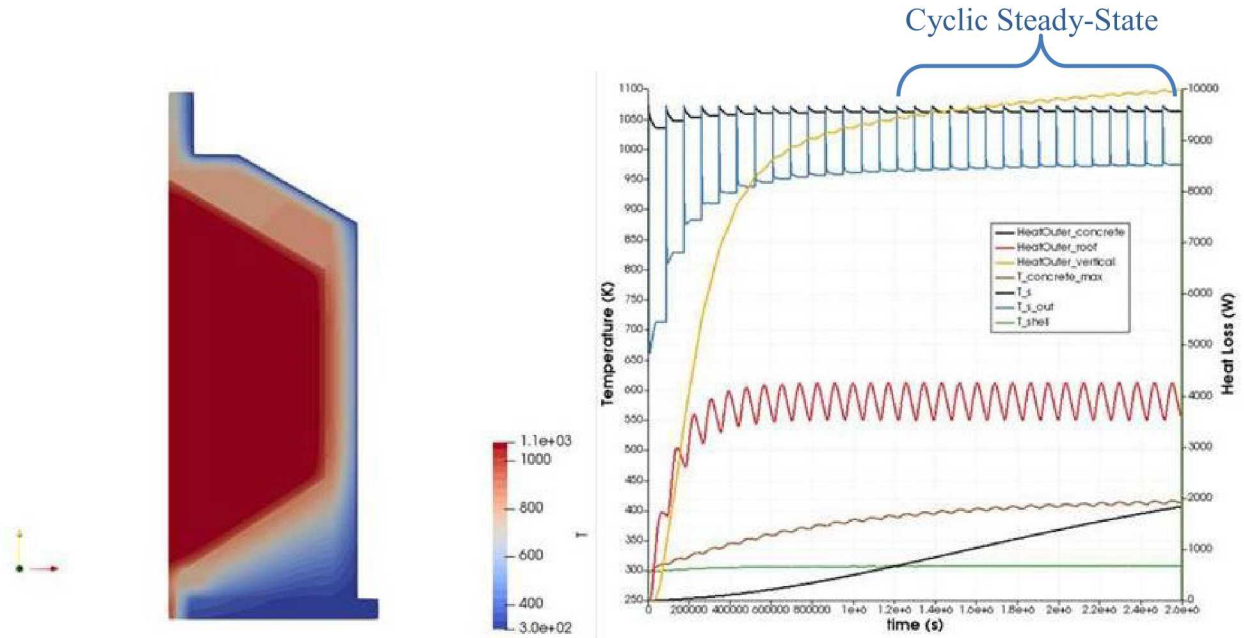

(a) (b)

Figure 2. Model parameters for cyclic thermal model. (a) Thermal contour across 2D axisymmetric cross section. (b) Results: Flux and heat through outer shell. T_s is the integrated average of all bulk solids. T_s_out is the integrated average temperature of the boundary layer between solid particles and the inner wall surface.

The cyclic steady-state models were also used to inform the extent to which changes in form factor and, consequently, surface area affect heat loss. Figure 3a shows an overlay of the average temperature of the bulk solids and Figure 3b shows the same information in terms of heat loss as a percentage of the 6MWh$_t$ duty. The average temperature of bulk solids dropped approximately 12-15°C over the 10-hour storage period after the refractory layers had come to cyclic steady-state. As expected as the bin becomes elongated and the surface area of the formation of the bulk solids increases, heat loss increases. However, the magnitude of this SA correlated increase is shown to be relatively minor. For a height to diameter ratio increase of 400%, the increase in heat loss is expected to be on the order of 1.2%.

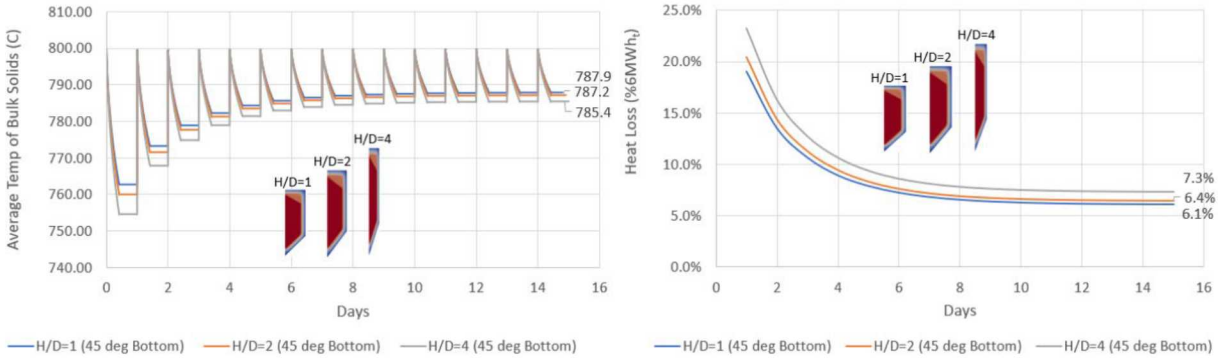

(a) (b)

Figure 3. (a) Daily cyclic steady-state temperature drops for three bin designs with increasing height/diameter (H/D) ratios of the cylindrical section of the particle formation and the current G3P3 flat-bottom design. (b) Daily cyclic steady-state heat loss as a percentage of 6MWh$_t$ capacity for the same bin designs.

Modeling Heat Loss in Dynamic Flow

Recalling that particle outlet temperatures can drop no more than 22° C after 8-hours of charging, 10-hours of storage, and 6-hours of discharging combined, a dynamic model was developed to characterize the thermal processes as cooler particles that remained in storage for 10 hours near the walls flow away from the walls along the drawdown cone and into the flow channel where they will mix and exchange heat with hotter particles surrounding the flow channel on the way to the outlet and eventually the heat exchanger.

Funnel Flow Properties

Funnel flow in bulk solids occurs when the slope of the hopper bottom is not steep enough to overcome wall-friction forces and particle motion along the wall ceases and only flows through a central flow channel. Hoppers are often designed with very steep inclines in order to ensure *mass flow* whereby all particles in the bin have the same vertical velocity. For applications involving CSP hot particle storage, the motion of particles along the wall is a risk for erosion of the refractory insulation liner and it may be desirable to utilize funnel flow designs to prevent motion along the walls. The characteristics of funnel flow design are defined by material properties of the particles and the wall surfaces. Flow property testing was performed by Jenike and Johanson to derive the effective angle of internal friction (δ) and kinematic angle of friction (ϕ) at 800° C. These properties, expressed as the angle between normal and resultant forces from shear cell testing on Mohr circles, are derivatives of measured particle to particle friction forces [3]. The drawdown angle defines the slope along which the particles slide from the wall into the flow channel and consequently, the angle of the residual particles in the bottom of the container. The drawdown angle is the average of δ and ϕ whose values are a function of both consolidating pressure and temperature. The flow channel angle (θ_f) is a function of δ and describes the cone angle from a projected cylinder normal to the outlet perimeter. Peter C. Arnold [4] gives this relationship as

$$\theta_f = 45° - 0.5\cos^{-1}\left(\frac{1-\sin(\delta)}{2\sin(\delta)}\right) \quad (1)$$

The result of temperature and pressure on flow channel angles in the G3P3 storage bin is estimated to decrease the flow channel angle from 12° at ambient temperature to 20° at high temperature as shown in FIGURE 4 and FIGURE 5.

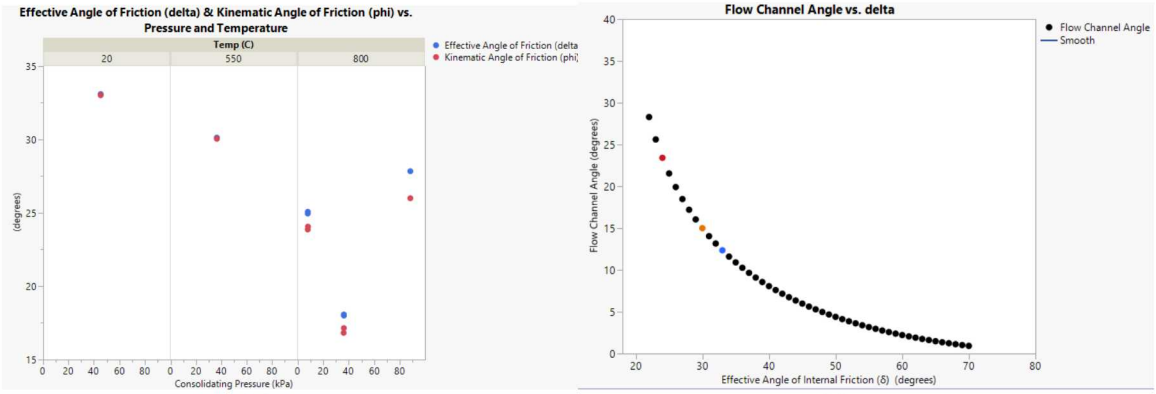

(a) (b)

FIGURE 4. (a) Effective angle of internal friction (δ) and kinematic angle of friction (ϕ) as measured at multiple levels of temperature and consolidation pressure. (b) flow channel angle as a function of δ calculated using Eq. 1. Values at the tested temperatures are colored to indicate relevant range: blue = 20° C, orange = 550° C, red = 800° C.

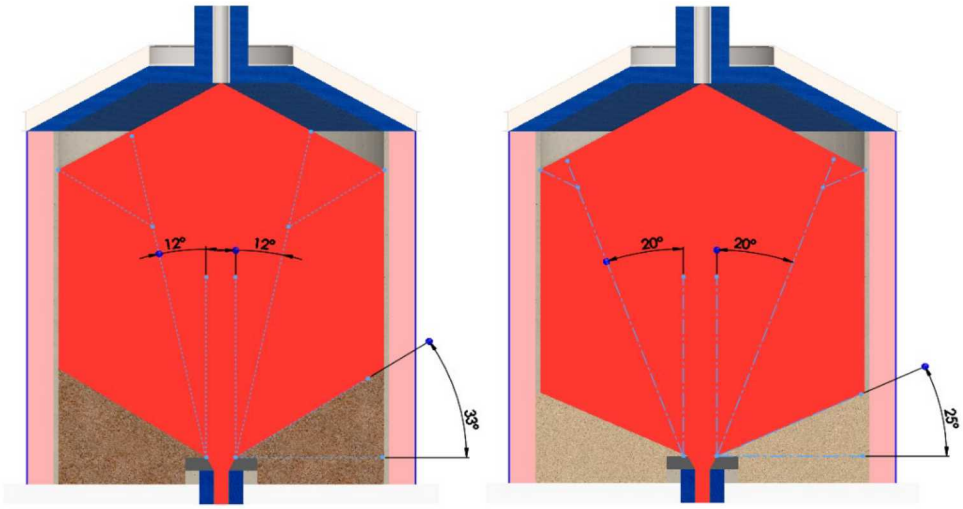

FIGURE 5. (a) estimated flow channel and drawdown angle at ambient temperature. (b) estimated flow channel and drawdown angle at 800° C

Level-Set Modeling

FIGURE 6 depicts the geometry of an axisymmetric model for flow and energy transport in a particle-filled bin. The flowing particles are treated as a pseudo fluid, and the flow and energy transport is modeled using conservation equations for flow and energy transport through a pseudo porous medium, with unit porosity.

The particle region is decomposed as a flowing powder region, the funnel flow, and a non-flowing, stationary powder region. The air-filled region above the particles is not modeled in the results below. The 3 regions are separated by level set interfaces with specified velocity to match the specified outflow of particles from the funnel flow region. The level sets separate the different fluid regions; each region allows individual flow and transport properties. The upper level set is the air/powder interface, set at the fixed "drawdown" angle, θ, measured from horizontal. The lower level set is the interface between flow and nonflowing powder. It has one leg at the same drawdown angle as the upper level set, which intersects a fixed (non-moving) third level set comprising the flow channel, set at an angle of 22° from vertical.

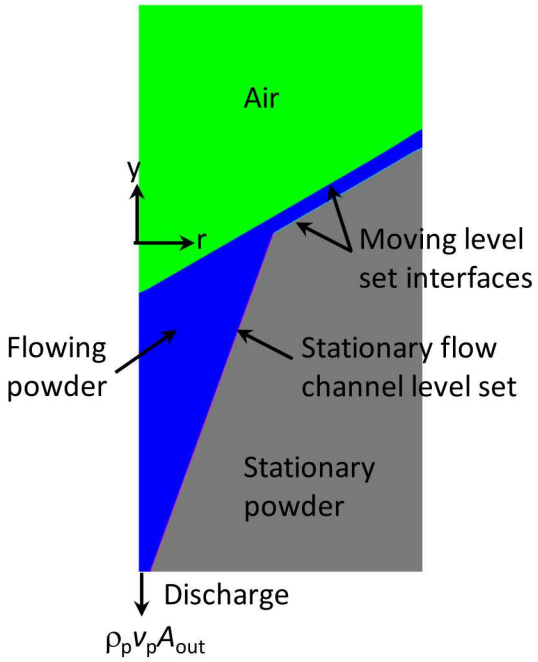

FIGURE 6. Axisymmetric particle bin geometry.

The particle region is enclosed in a thin metal bin (not shown) with convection and radiation boundary conditions applied at the outer surface. The initial temperatures are prescribed from the experiment, as is the initial mass in the bin. The flow is driven by specifying the discharge rate out of an orifice at the bottom of the bin; the level sets move downward at a uniform speed set to match the discharge rate. The drawdown region convects cold particles at the wall toward the flow cone and out the discharge orifice. The main purpose of the model is to predict the cooling of particle discharge with time.

Figure 7 shows the results of the preliminary G3P3 1 MW_t simulation. Outlet temperatures are shown to drop about 6-7 degrees over the 6 hours of flow.

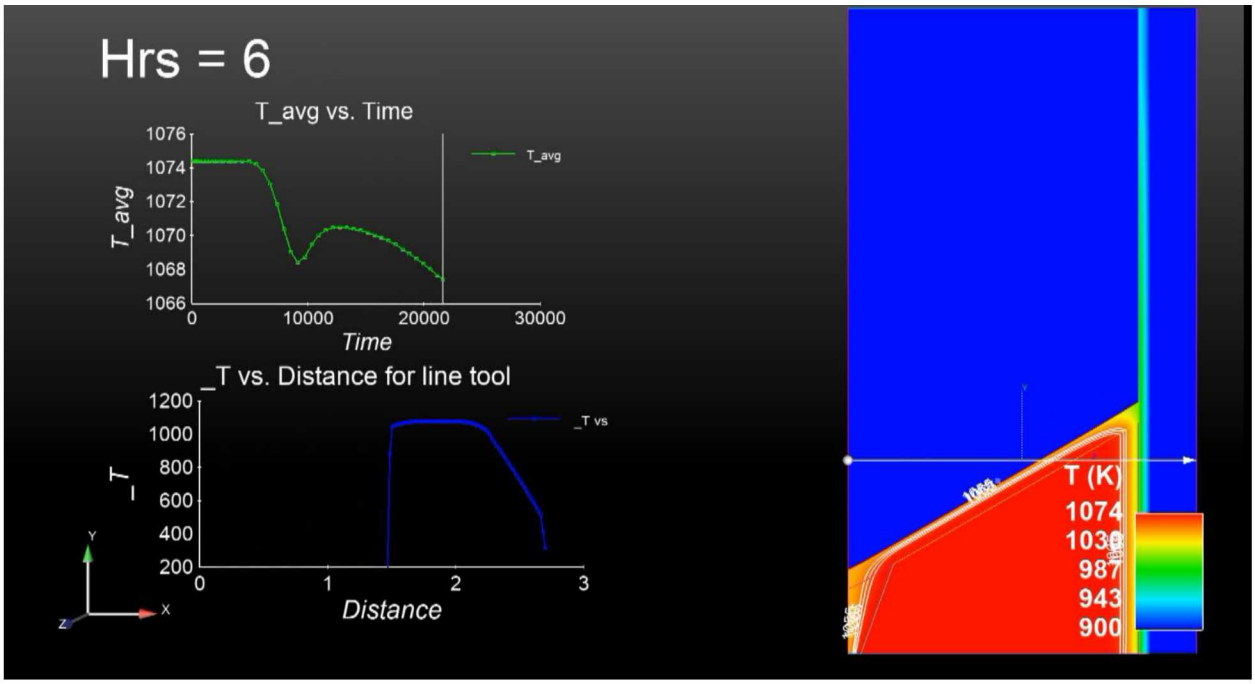

FIGURE 7. Level-set modeling results of the G3P3 1 MW_t particle storage bin.

TESTING

The objective of this test is to provide measurements of particle temperatures throughout a particle bin that is heated and discharged similarly to the G3P3 hot particle storage bin currently being designed. A small particle bin was filled with CARBO HSP 40/70 particles. The bin was heated to 800° C in a furnace until all particles were brought to equilibrium. The bin was removed from the furnace and left outdoors to cool until temperature gradients formed between temperatures at the wall and in the center of the bin. A slide gate beneath the bin was then opened to allow particles to flow out of the bin. Thermocouples (TCs) were mounted along the inside wall and center of the bin. Three TCs were positioned just above the outlet hole. Data was logged continuously as the particles flowed out of the bin. A scale was placed under a catch bin to measure the flowrate. Figure 8a shows the basic test configurations. Item 1 is the test bin which includes a steel frame that was necessary to allow extraction from the furnace with a forklift. The slide gate is attached to the bottom and surrounded by insulation to reduce convective and advective losses around the outlet. A washer-like disk was placed in the outlet pipe to ensure plugged flow below the outlet hole and minimize air entrainment in the results. Item 2 is the catch bin which is placed on a scale. Items 3a-c are the locations of TCs placed to capture ambient air temperatures 3 meters from the bin. Item 4 is an anemometer which provided data to derive convective heat transfer coefficients. Figure 8b shows the placement of TCs inside the bin.

(a.) (b.)

Figure 8. (a.) Test configuration: 1, hot particle test bin. 2, catch bin. 3a-c, ambient thermocouples. 4, anemometer. 5, scale. (b.) Thermocouple placement: 6, wall TCs 1-4 from top to bottom. 7, center TCs 1-3 from top to bottom. 8, outlet TCs 1-3

Test Results

Figure 9 shows the measured temperatures (blue) from a TC near the wall. The model (black) was calibrated by adjusting the emissivity and conduction coefficient to match the falling wall temperatures. The empirical data was shifted in time such that the slide gate was opened at t=0 while the model timing was adjusted forward in time to allow the drawdown cone to develop in the test bin so particle levels along the wall and mass would match.

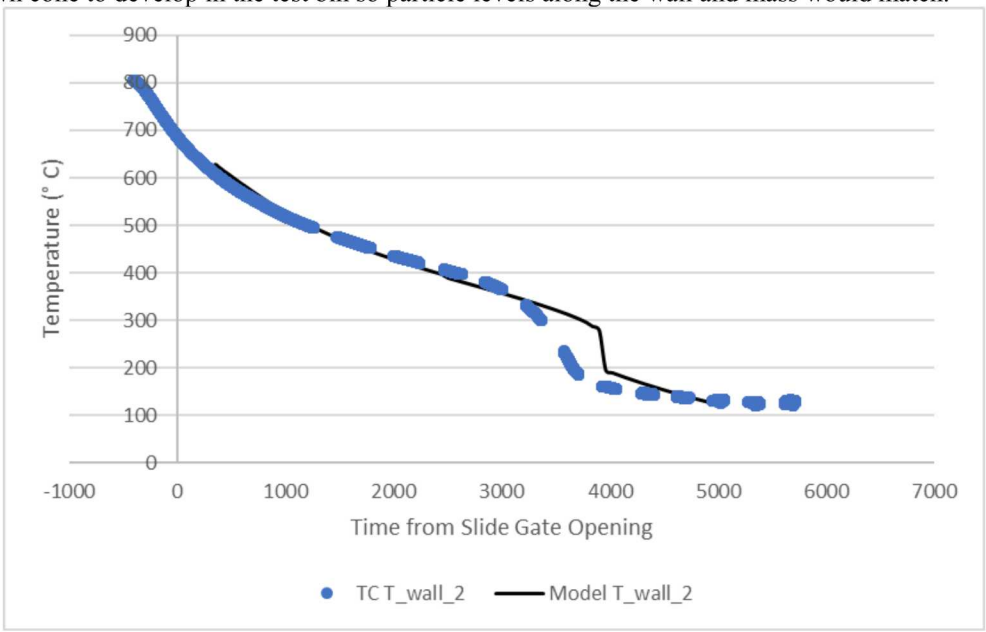

FIGURE 9. Measured wall temperatures overlaid with model output fit to data. Data is adjusted in time so that the slide gate opened at t=0. Model data is adjusted forward in time to allow test particles to form drawdown cone.

FIGURE 10 presents an overlay of outlet thermocouple data and the model data. Both show a relatively large variation. The model probed at the center of the outlet hole and 3 mm from the edge of the outlet hole. Two of the test TCs (CL1 and CL2) hovered about 3 mm above the center of the outlet hole and the third outlet TC, TC_T_out_edge was bent so that the tip would be near the edge of the outlet hole. The results indicate the model is

capturing the overall temperature profile over time. However, the test temperatures are about 100° C lower than the model predicts. The model did not account for heat conduction through the slide gate and the steel frame around the bin. The model also did not account for radiation from the particle bed surface to the container lid. Other advective losses in the outlet may not have been captured. Sensitivity studies on the effect of flow channel and drawdown angles have not been performed so it is not known how discrepancies in these parameters may affect outlet temperatures.

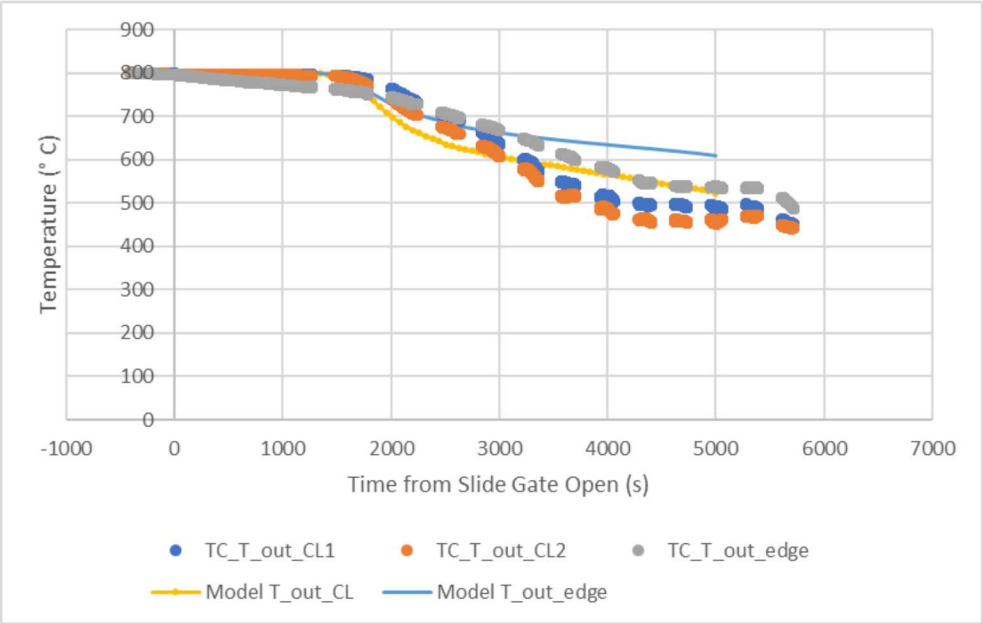

FIGURE 10. Overlay of modeled and measured TC temperatures at outlet.

SCALABILITY

Designs for a particle storage bin that would provide 14 hours of energy storage for a 100 MW_e system with a 50% thermal to electric conversion efficiency were evaluated. Using equations 2 and 3, the required flow rate is ~1 kiloton per second and the total bulk mass for 14 hours (50,400 s) of heat transfer is 54.3 million kg. The total mass including 15.3 kiloton of stagnant particles would be 69.6 kiloton. In the minimum SA configuration, the diameter would be 34.76 m the height of the bin interior would be 40.29 m and the total interior volume would be 34.6 m^3.

$$\dot{m} = \frac{200E^{-6}}{1243\frac{\mathrm{J}}{\mathrm{g*K}}*160°\,\mathrm{K}} = 1000.6\,\frac{\mathrm{kg}}{\mathrm{s}} \tag{2}$$

$$\int_0^{50,400} m\,dt = 100.6\frac{kg}{s}(50{,}400s) = 54{,}310{,}346\ \mathrm{kg} \tag{3}$$

Figure 11 calculates changes in surface area (SA) of the formation of flowing particles, maximum vertical stress on the wall at an element located at floor level, and maximum wall tension at floor level as the height to diameter (H/D) ratio of the cylinder portion of the particle formation is elongated. At each iteration, the diameter is increased thus defining the drawdown and surcharge geometries and the height is then set to maintain constant mass of the flowing portion of particles. The H/D ratio indicates the ratio of the bin diameter to the height of the cylindrical portion excluding the drawdown and surcharge heights. The resulting bin height in the bottom abscissa is of the entire particle formation including the drawdown and surcharge. The vertical stress is calculated with the Janssen equation (Eq. 4) which accounts for the supportive particle to particle friction forces that transfer some of the vertical loads to the walls of the silo thus relieving the stress acting on the bottom of the tank by an increasing amount as the bin elongates. However, as the bin diameter decreases, the area of the floor decreases by a power of 2. For this reason,

the stress on the floor initially rises until an H/D ratio of about 2 where after the Janssen forces begin to dominate. Not shown is the horizontal stress which can be assumed to be about 40-60% of the vertical stress, and the shear stress which is calculated as the horizontal stress times the wall friction coefficient (μ_w) where, $\mu_w = \tan(\phi')$. ϕ' is the wall friction angle which was measured empirically. The average value of μ_w from the top to the bottom of the bin was found to be ~0.5 at operational temperatures. The wall tension is the product of the horizontal force and the bin radius. Wall tension decreases monotonically with diameter but as bins reach heights over 50 meters seismic shear and overturning moments begin to dominate requiring a substantial amount of reinforced concrete. Dome style external storage bins are the most cost-effective solution for commercial scale storage. Receiver tower integrated storage is feasible but only in regions with minimal seismic activity.

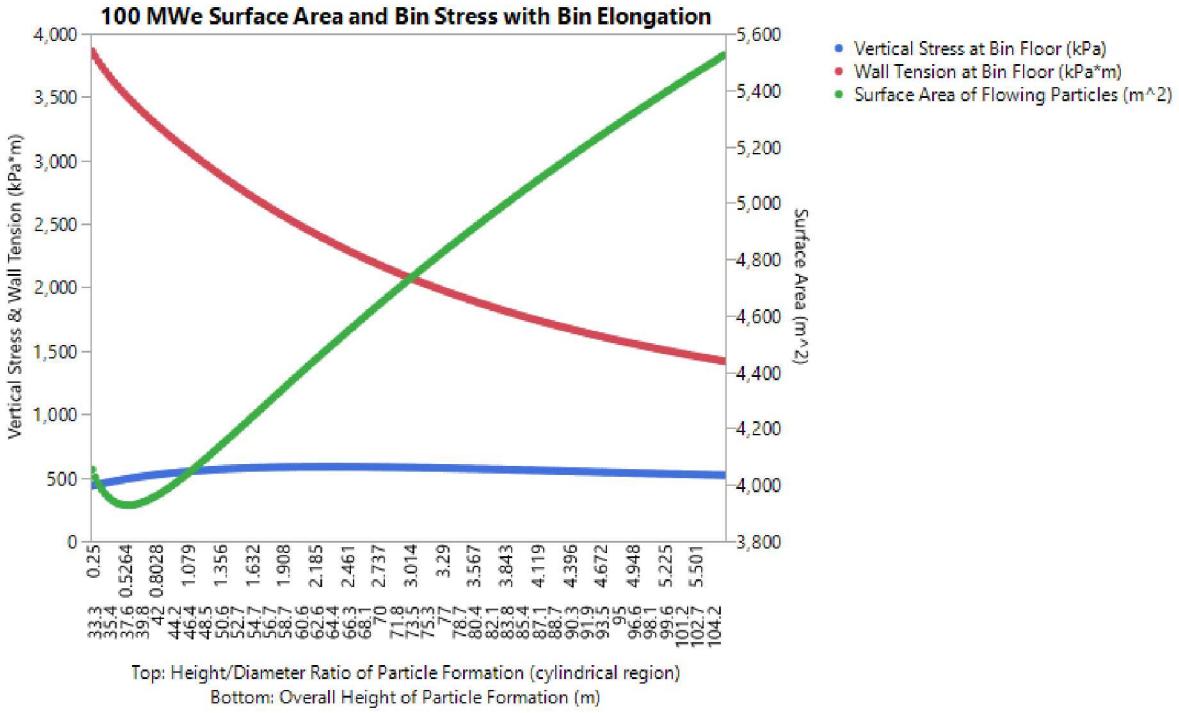

Figure 11. Vertical stress, wall tension, and surface area of a 100 MW_e storage bin as a function of height/diameter ratio. Corresponding overall bin height is shown in lower abscissa.

Heat Loss Modeling for 100 MW_e Systems

Three primary considerations were made regarding heat loss characteristics of commercial scale systems: 1, what is the effect of elongation, and by extension increased surface area, on heat loss? 2, given the size of the storage vessels, how much does insulation affect the overall heat loss? 3, is the technoeconomic benchmark of a <1% heat loss relative to 2800 MWh_t achievable?

The same cyclic steady-state model was run on 100 MW_e bin designs with minimum SA, 100 m height, and 200 m height. The height of 200 m was chosen as a maximum height that might be available in a receiver tower designed for integrated storage. In these models the same insulation configuration as the G3P3 1MW_t bin was applied for the sake of comparison. This insulation configuration would likely be cost prohibitive and a shotcrete or gunnite type application would be necessary. To evaluate how much of the thermal resistance is attributable to the particle formation vs. the insulation, the minimum SA geometry was rerun without insulation.

FIGURE 12 gives an overlay of the results. The final temperatures and heat loss as a percentage of the 200MW_t duty is labeled. As expected, heat loss increases with elongation. For an increase in height of 400% (40 m to 200 m) heat loss increased by 0.5%. The contribution of insulation was evaluated and shows an increase in heat loss between the insulated and uninsulated minimum SA bin to be 2.5%.

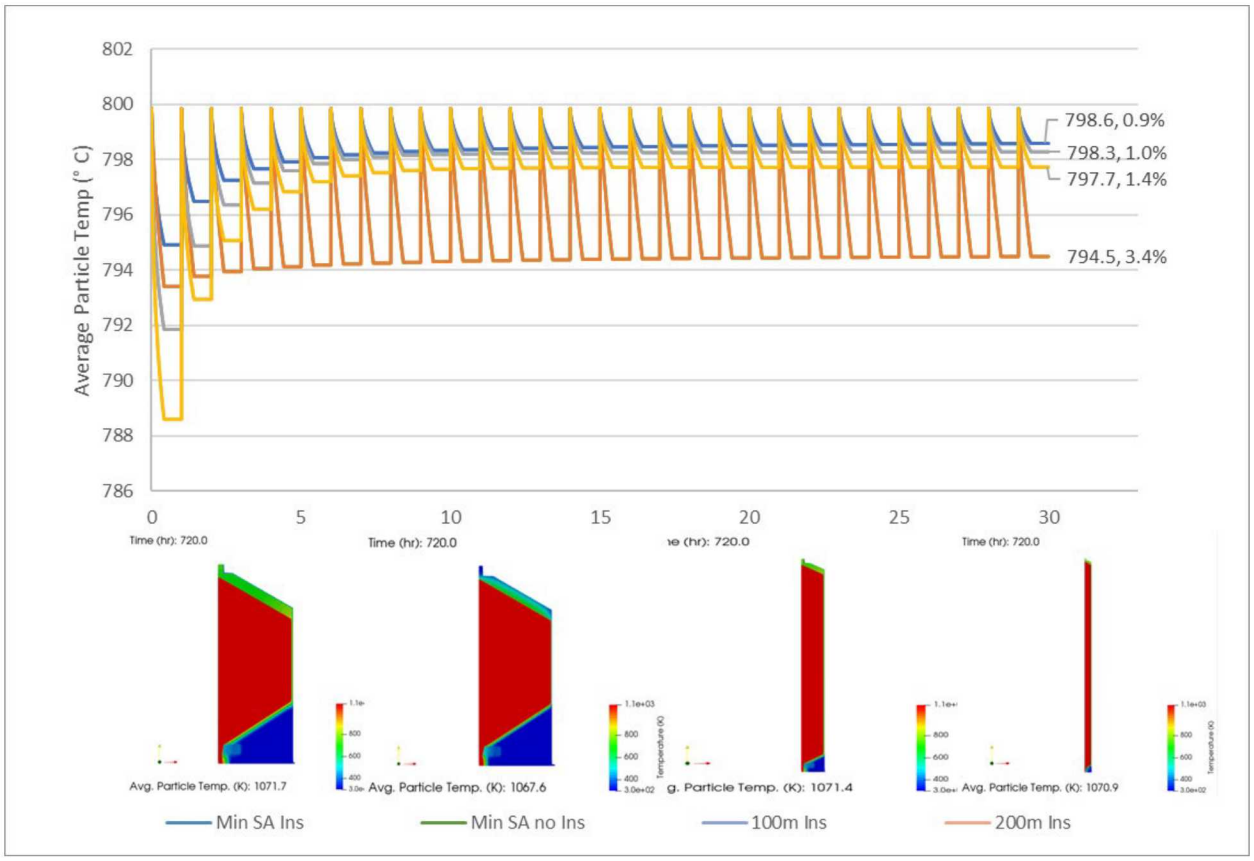

FIGURE 12. Cyclic average particle temperatures for four bin concepts with final temperature and heat loss as a percentage of a 160° ΔT needed for 200MW$_t$. Contour plots portray relative form factor of the particle formations.

CONCLUSIONS

The self-insulating properties of dense ceramic particles such as CARBO HSP may be advantageous in CSP storage applications. Cyclic steady-state modeling indicates that the stagnant region of particles that would remain on the floor of flat-bottomed bins may reduce the need for insulation along the area of the floor. The same models indicate that after 14 hours of deferred storage, insulation reduces heat loss by 2.5% more than uninsulated bins of similar geometry relative to the 200 MW$_t$ duty indicating that the particles themselves account for most of the thermal resistance in the system. There is a tradeoff between bin stresses and thermal losses. As silos elongate, the Janssen effects reduce vertical and horizontal stress but increase surface area. Modeling shows that at both the 1 MW$_t$ and 200 MW$_t$ scales, elongation has by 400% increases heat loss by 1.2% and 0.5% respectively during deferred storage. Stress calculations based on the Janssen equation indicate that the 1 MW$_t$ bin can survive hydrostatic stress with ample margin. The 200 MW$_t$ design may also sustain hydrostatic stresses, but the seismic shear and overturning moments may preclude the use of elongated storage structures and need to be further investigated in future work. Ground based storage structures may be more cost effective.

Total heat loss of the storage system includes both the charging, deferred storage, and discharge phases. Insulation design and system performance predictions can be improved if the temperature drop over the charging and discharging phase is known. To this end, a method was developed using geometric computation level-sets to model the thermal characteristics of particles in funnel flow. To validate this model, a small scale flat-bottom particle bin was heated to operating temperatures and allowed to drain. Comparisons of model and test data show that many salient characteristics of the thermal exchange are captured. However, more work is needed to build confidence that this approach can accurately predict the outlet temperatures of the small test bin. Current dynamic modeling of the G3P3

bin predicts temperatures will drop on the order of 6 to 7 degrees Celsius. This value is preliminary and may be refined as it is informed by validation testing.

Future work may incorporate radiation of the particle bed surface to the metal bin interior. Modifications of the test bin or model may improve results by capturing the effects of conduction in key places around the bin. Sensitivity studies on flow channel and drawdown angles may help inform whether these parameters require additional scrutiny. Models will be used to compare heat loss characteristics of funnel flow vs. mass flow bin designs.

ACKNOWLEDGEMENTS

This work is funded in part or whole by the U.S. Department of Energy Solar Energy Technologies Office under Award Number 1497.

REFERENCES

1. Clifford K. Ho, K.A., Lindsey Yue, Brantley Mills, Jeremy Sment, Joshua Christian, Matthew Carlson, *Overview and Design Basis for the Gen 3 Particle Pilot Plant (G3P3).* SolarPACES 2019 Conference Proceedings, 2019.
2. Albrecht, K.J., Clifford K. Ho, *Design and operating considerations for a shell-and-plate, moving packedbed, particle-to-sCO2 heat exchanger.* Solar Energy, 2018. **178**(January 2019): p. 331-340.
3. Mehos, G., *Hopper Design Principles for Chemical Engineers*. Kearney, NE: Morris Publishing.
4. Arnold, P.C., *Bulk Solids Handling*. 1980: TUNRA Bulk Solids Handling Research Associates.